Miller, M. R., Seighman, C., & Ulrich, R. G. (1985b) *Biochemistry 24*, 7440–7445.
Nishida, C., Reinhard, P., & Linn, S. (1988) *J. Biol. Chem. 263*, 501–510.
Pedrali-Noy, G., & Spadari, S. (1979) *Biochem. Biophys. Res. Commun. 88*, 1194–1202.
Plevani, P., Badarocco, G., Ginella, E., & Sora, S. (1980) *Antimicrob. Agents Chemother. 18*, 50–57.
Prelich, G., Kostura, M., Marshak, D. R., Mathews, M. B., & Stillman, B. (1987a) *Nature 326*, 471–475.
Prelich, G., Yan, C.-K., Kostura, M., Mathews, M. B., So, A. G., Downey, K. M., & Stillman, B. (1987b) *Nature 326*, 517–520.
Roberts, J. J. (1978) *Adv. Radiat. Biol. 7*, 212–436.
Ross, S. L., & Moses, R. E. (1976) *Antimicrob. Agents Chemother. 9*, 239–246.
Scovassi, A. L., Plevani, P., & Bertazzoni, U. (1980) *Trends Biochem. Sci. (Pers. Ed.) 5*, 335–339.
Tan, C.-K., Castillo, C., So, A. G., & Downey, K. M. (1986) *J. Biol. Chem. 261*, 12310–12316.
Tanaka, S., Hu, S.-Z., Wang, T. S.-F., & Korn, D. (1982) *J. Biol. Chem. 257*, 8386–8390.
Tseng, B. Y., & Goulian, M. (1975) *J. Mol. Biol. 99*, 317–337.
Vishwanatha, J. L., Coughlin, S. A., Weslowski-Owen, M., & Baril, E. F. (1986) *J. Biol. Chem. 261*, 6619–6628.
Wahl, A. F., Crute, J. J., Sabatino, R. D., Bodner, J. B., Marracino, R. L., Harwell, L. W., Lord, E. M., & Bambara, R. A. (1986) *Biochemistry 25*, 7821–7827.
Wilson, S., Abbotts, J., & Siden, S. (1988) *Biochim. Biophys. Acta 949*, 149–157.
Wist, E., & Prydz, H. (1979) *Nucleic Acids Res. 6*, 1583–1590.
Wright, G. E., & Dudycz, L. W. (1983) *J. Med. Chem. 27*, 175–181.
Yagura, T., Kozu, T., & Seno, T. (1982) *Eur. J. Biochem. 123*, 15–21.
Zimmerman, W., Chen, S. M., Bolden, A., & Weissbach, A. (1980) *J. Biol. Chem. 255*, 11847–11852.
Zmudzka, B. Z., Fornace, A., Collins, J., & Wilson, S. H. (1988) *Nucleic Acids Res. 16*, 9587–9596.

Enthalpic and Entropic Contributions to Actin Stability: Calorimetry, Circular Dichroism, and Fluorescence Study and Effects of Calcium†

A. Bertazzon, G. H. Tian, A. Lamblin, and Tian Yow Tsong*
Department of Biochemistry, University of Minnesota College of Biological Sciences, St. Paul, Minnesota 55108
Received May 16, 1989; Revised Manuscript Received August 23, 1989

ABSTRACT: The ΔH associated with the thermal unfolding of G-actin has been determined by differential scanning calorimetry (DSC) to be 142 ± 5 kcal/mol, with the T_m (melting temperature) at 57.2 ± 0.5 °C, at pH 8.0 (heating rate 0.5 K/min). The transition is broad and cannot be treated as a single transition that mimics a two-state process, suggesting the existence of domains. Deconvolution is done to fit it into two quasi-independent two-state transitions. For F-actin, the transition is more cooperative, with a cooperative ratio (the ratio of van't Hoff enthalpy and calorimetric enthalpy) of 1.4, indicating intermonomer interaction. The ΔH of the thermal unfolding of F-actin is 162 ± 10 kcal/mol with a T_m at 67.0 ± 0.5 °C. A state of G-actin similar to that of the heat-denatured form, designated D-actin, is obtained by removing tightly bound Ca^{2+} with EGTA. The DSC-detectable cooperative transition is completely lost when the free calcium concentration of the medium is 1×10^{-11} M or lower, using a Ca^{2+}/EGTA buffer system. However, circular dichroism (CD) shows that the helix content of actin, 32% in the G-form, is only partially reduced to 19% in this apo form. The CD spectrum and the helix content of the calcium-depleted actin are almost identical with those of the heat-denatured D form. This loss of 40% of the native helical content is irreversible in both cases. The remaining 60% of the native helical content cannot be further eliminated by heating to 95 °C. A complete and reversible unfolding of the D-actin can be obtained by 5 M guanidinium chloride or 8 M urea. The heat denaturation as well as chemical denaturant unfolding have also been followed by the intrinsic fluorescence of tryptophans. A red shift of the emission maximum from 325 to 335 nm is observed with heat and EGTA denaturation. Completely unfolded actin has an emission maximum at 345 nm. The accessibility of hydrophobic binding sites upon heat and EGTA denaturation is detected by ANS (anilinonaphthalenesulfonate) binding; the total number of binding sites increases by about 5-fold upon denaturation. These findings suggest a two-step pathway for the complete unfolding of G-actin, $N \rightarrow D \rightleftharpoons U$, where N, D, and U denote the native, a denatured but compact, and the completely unfolded states, respectively. The first irreversible step is characterized by a large enthalpic change and involves the dissociation of the high-affinity Ca^{2+}. This transition involves melting of two independent domains. The second reversible step is purely entropic and cannot be induced by heating. The structural characteristics of D-actin are intermediate between N- and U-actin. ΔG, ΔH, and ΔS of each conformational transition are given.

The folding–unfolding transition of small globular proteins is highly cooperative and approaches the two-state process [for a recent review, see Privalov and Gill (1988)]. For proteins with larger molecular weights or complex structures, the presence of independent cooperative domains can be detected or deduced from the analysis of calorimetric data (Privalov, 1982; Sturtevant, 1987). Recent studies of the thermal stability of proteins (Baldwin, 1986; Privalov & Gill, 1988) in-

† This work was supported by NIH Grant GM 37304.

0006-2960/90/0429-291$02.50/0

dicate that there is a temperature range (between cold and heat denaturations) in which stabilizing forces, such as van der Waals interactions and hydrogen bonding, overcome the dissipative forces of the hydration of nonpolar residues. The transition enthalpy, measured calorimetrically, is believed to originate from van der Waals interactions and hydrogen bonding in the protein structure.

The presence of residual structures in "unfolded" proteins, particularly in heat-denatured proteins, has been known (Tanford 1968). Unfortunately, attempts to distinguish between a partially unfolded protein (with residual structures) and the fully unfolded protein (e.g., the guanidinium chloride unfolded form) or to characterize these forms have been difficult (Privalov & Gill, 1988). Actin appears to be a good system for studying these questions. The heat-denatured actin (D-actin) retains approximately 60% of its native helical content as observed by ORD (optical rotatory dispersion) and CD (Nagy & Jenks, 1962; West et al., 1967; Nagy & Strzelecka-Golaszewska, 1972; Strzelecka-Golaszewska et al., 1985). A similar state of protein is obtained by removing tightly bound Ca^{2+}. Both processes result in a red shift of 10 nm for the Trp fluorescence emission which is consistent with only a partial exposure of tryptophan residues to the aqueous environment (Lehrer & Kerwar, 1972). Complete unfolding by 5 M guanidinium chloride and 8 M urea, and thus the exposure of tryptophan residues, results in a further red shift of 10 nm. We report here a systematic study of heat and EGTA denaturations, characterization of these denatured states, and comparison with the guanidinium chloride unfolding reaction. The enthalpy and entropy of each reaction are calculated and their contributions to the stability of proteins assessed.

Materials and Methods

Actin Purification. Actin was purified from acetone powder of muscle from New Zealand white male rabbits as described by Pardee and Spudich (1982). The procedure was modified by replacing Tris-HCl with HEPES (HEPES, 2 mM, pH 8.0; NaATP, 0.2 mM; $CaCl_2$, 0.2 mM; and mercaptoethanol, 0.5 mM) for any measurement involving heat denaturation. G-Actin was polymerized to F-actin by raising the concentration of NaATP to 1 mM and by adding 50 mM KCl and 2 mM $MgCl_2$ to the previous buffer. Formation of filaments was monitored by using electron microscopy. The purity of the protein was checked by SDS–polyacrylamide gel electrophoresis (PAGE), as described by Laemmli (1970), using a Bio-Rad miniprotean II system. The protein concentration was determined by UV absorption ($E^{1\%}_{290} = 6.3$) for G-actin. The concentration of F-actin was obtained by determination of the nitrogen content as described by Lowry et al. (1951).

Differential Scanning Microcalorimetry. DSC was performed with a MC-2 scanning calorimeter (Amherst, MA) interfaced to an AT & T PC 6300 personal computer through an A/D converter (DT 2801 board). The software was provided by the manufacturer as a data acquisition package (EMF software). The data analysis of this package is based on the deconvolution procedure of Freire and Biltonen (1978a–c). In this procedure, the partition function of the system is directly obtained from DSC data, and a DSC spectrum can be resolved into either multiple independent or sequential two-state processes. The capacity of the calorimeter cell is 1.241 mL, and all the available heating rates, between 0.16 and 1.5 K/min, were used. Proteins were dialyzed overnight against the reference buffer, and concentrations ranging from 1.2 to 13 mg/mL were used, with no noticeable effect on the enthalpy and T_m. Baselines were drawn as a straight line from the T_i to the T_f of the transition, the two temperatures being the initial and the final temperatures, respectively, for analysis from a DSC curve (Takahashi et al., 1981). The van't Hoff enthalpy was calculated by means of the partition function Q (Privalov & Potekhin, 1986): $\Delta H_{vH} = RT^2[d(\ln Q)/dT]$. In a fluorescence study, ΔH_{vH} was calculated from equilibrium constant by using the van't Hoff equation. The cooperative ratio (CR) is defined here as $\Delta H_{vH}/\Delta H_{cal}$, and values higher than 1 are interpreted as effects due either to aggregation or to intermolecular interaction, whereas a lower value suggests the presence of a multidomains transition (Privalov & Pothekin, 1986; Tsong et al., 1972).

Circular Dichroism. The ellipticity of the protein was followed by using an AVIV 60 DC spectropolarimeter interfaced to an AT & T PC 6300 personal computer (at the Johns Hopkins University) or alternatively with a Jasco J 41 C spectropolarimeter interfaced through an Adalab A/D converter to an IBM-XT compatible personal computer. Water-jacketed, thermostated quartz cells were obtained from Hellma (Forest Hill, NY) with path lengths of 1 and 0.1 mm. Calibration of the instruments was done with (+)-10-camphorsulfonic acid. The temeprature of the sample was followed in the cell by using a previously calibrated YSI 511 microprobe. Protein concentrations of 0.5–1 mg/mL were used. CD is expressed as the mean ellipticity per residue, $[\theta] = \theta^\circ \cdot MRW/cl$, which has dimensions of degree centimeter squared per decimole and where the mean residue weight (MRW) of 115 was used (Nagy & Strzelecka-Golaszewska, 1972). c represents the protein concentration in grams per milliliter, and the light path of the quartz cell is l.

Fluorescence Measurements. The intrinsic fluorescence of the protein and ANS (1-anilino-8-naphthalenesulfonate) was followed by using an Aminco–Bowman spectrophotofluorometer (Silver Spring, MD). Intrinsic fluorescence was measured by using 290 nm as the excitation wavelength and 335 nm as the emission wavelength. For ANS fluorescence, the excitation and the emission maxima were 400 and 470 nm, respectively, in the buffer used for actin. Binding constants were obtained from the titration curve by using Scatchard analysis. ANS was allowed to react with protein for 10 min for each data point. Where fluorescence spectral shifts were to be monitored, a Perkin-Elmer MPF 44A fluorescence spectrophotometer was used. Melting curves were obtained with a continuous temperature programmer by Neslab which controlled a Lauda K2/RD water circulator. The sample temperature was directly measured with a thermistor probe.

Urea and Guanidinium Chloride Denaturation. Ultrapure guanidinium chloride (enzyme grade) was obtained from Bethesda Research Laboratories (Gaithersburg, MD), and electrophoresis purity urea was obtained from Bio-Rad (Richmond, CA). When reversibility was to be checked, the denaturant was removed by dialysis at 4 °C for 12 h. The free energy of denaturation was calculated by linear extrapolation to zero denaturant concentration as previously described (Pace, 1975; Tanford, 1968).

Calcium Determination. The free Ca^{2+} concentration in the EGTA/Ca^{2+} buffer system was calculated according to Tsalkova and Privalov (1985) using an association constant of 5.0×10^{10} M^{-1} (Schmid & Reilley, 1957). The change in the number of bound Ca^{2+} (Δn) upon thermal unfolding was determined from calorimetric data by using the following procedure. The binding is assumed to be a single-step process represented by the equation:

$$A + \Delta n Ca^{2+} = A \cdot \Delta n Ca^{2+}$$

where A is actin. The apparent equilibrium constant, K_{app},

is given by

$$K_{app} = \frac{[A \cdot \Delta n Ca^{2+}]}{[A][Ca^{2+}]^{\Delta n}}$$

The fraction of protein with high-affinity calcium, α, is

$$\alpha = \frac{[A \cdot \Delta n Ca^{2+}]}{[A] + [A \cdot \Delta n Ca^{2+}]}$$

Calorimetrically, α is simply the enthalpy measured at a specific calcium concentration divided by the enthalpy measured at a saturated calcium concentration. It can be shown, then, that

$$\log [\alpha/(1 - \alpha)] = \log K_{app} + \Delta n \log [Ca^{2+}] \quad (1)$$

Thus, from the slope of a plot shown in Figure 3B, Δn can be obtained.

The release of Ca^{2+} from heat-denatured D-actin was determined by the method described by Kendrick et al. (1977). Free calcium chelates with Arsenazo III, [2,2'-(1,8-dihdyroxy-3,6-disulfonaphthylene-2,7-bis(azo)bisbenzenearsonic acid]. Arsenazo III, in the form of sodium salt, was obtained from Sigma (St. Louis, MO). The following spectroscopic method was used to obtain its concentration from a calibration curve. The protein was dialyzed overnight for complete removal of unbound Ca^{2+}. Standard calibration wad done in the dialysis buffer using 2.5–25 μmol of protein. Each sample wad divided into two parts; one was untreated, and the other was heated at 60 °C for 30 min and then rapidly cooled. Calcium values determined for native and heat-denatured protein were 1.6 ± 0.3 and 2.57 ± 0.1 M/M, respectively. The number of Ca^{2+} released was 0.97 M/M. This result does not exclude the possibility that there is calcium which after being released from its native sites still binds to the protein with an affinity higher than that of the chelating constant of Arsenazo III, as is suggested from the data of Figure 3B.

Results

Heat Denaturation of N-Actin. The thermal denaturation of G-actin is apparently irreversible (on the basis of enthalpy changes) and is a relatively slow reaction. Thus, in comparing the DSC result, it is important to define experimental conditions precisely. Unless otherwise specified, a heating rate of 0.5 K/min was used in these experiments. Figure 1A shows the excess heat capacities for G-actin (4.3 mg/mL) and F-actin (4.8 mg/mL) upon thermal denaturation. The calorimetric ΔH thus obtained was 142 ± 5 kcal/mol at a T_m of 57 ± 0.3 °C for G-actin and 162 ± 10 kcal/mol at a T_m of 67 ± 0.5 °C for F-actin. The equilibrium thermodynamic analysis was used to obtain these enthalpy values despite the fact that these thermal transitions are apparently irreversible. This has been done previously in order to gather useful information for understanding the denaturation process (Tatunashvili & Privalov, 1984; Edge et al., 1985; Privalov & Potekhin, 1986). In panels B and C of Figure 1, experimental curves are compared with theoretical curves, assuming a two-state transition, with the parameters listed in Table I for G-actin and F-actin, respectively. The cooperative ratio is less than 1 (0.7) for G-actin, suggesting that the denaturation is not a simple two-state process, and therefore can be resolved into multiple steps. Fitting of the excess heat capacity curve into two independent two-state steps is shown in Figure 1D. The best fit was obtained with two transitions, one at a T_m of 52.3 °C with a ΔH_{cal} of 44 kcal/mol and the other at a T_m of 56.7 °C with a ΔH_{cal} of 107 kcal/mol. Fitting to a two sequential two-state process was also attempted, and the values are also reported in Table I. The resolution into two independent melting processes is appealing because the enthalpy values for the two transitions are proportional to the molecular weights of the two fragments obtained after limited proteolysis of G-actin (Jacobson & Rosenbush, 1976). Thermodynamic quantities were calculated by the procedure of Privalov et al. (1986) and are listed in Table I. The endotherm of F-actin is much sharper than that of G-actin, with a CR (cooperative ratio, i.e., $\Delta H_{vH}/\Delta H_{cal}$) of 1.4, and the T_m is shifted to 67 ± 0.5 °C. The higher cooperativity and greater stability of F-actin are related to the formation of filamentous structures.

Effects of Calcium on the Enthalpy of Denaturation. In Figure 2, the effect of calcium on the ΔH_{cal} of heat denaturation is examined. The $[Ca^{2+}]$ was controlled with a Ca^{2+}/EGTA buffer system. The protein was dialyzed overnight (or at least 12 h) against a Ca^{2+}/EGTA solution with a known free calcium concentration, at 4 °C, and DSC was

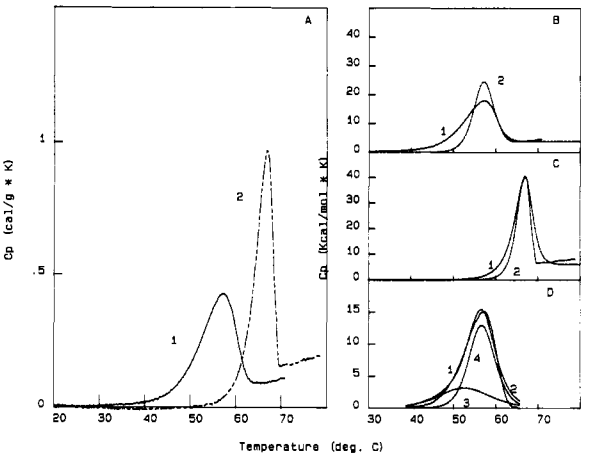

FIGURE 1: Calorimetric melting curves of G- and F-actin. (Panel A) Curve 1, G-actin, 4.3 mg/mL, in 2 mM HEPES, 0.2 mM ATP, 0.2 mM $CaCl_2$, and 0.5 mM mercaptoethanol at pH 8.0; curve 2, 4.8 mg/mL F-actin in 2 mM HEPES, 1 mM ATP, 50 mM KCl, 0.2 mM Ca^{2+}, 2 mM $MgCl_2$, and 0.5 mM mercaptoethanol at pH 8.0. The scanning rate was 0.5 K/min in both cases. (Panel B) Comparison of the DSC endotherm of G-actin (1) with the simple two-state transition (2) using a ΔH of 140 kcal/mol and a T_m of 57.0 °C, based on the van't Hoff equation. (Panel C) Comparison of the endotherm of F-actin (1) with the simple two-state transition (2) using a ΔH of 180 kcal/mol and a T_m of 67.2 °C. The calorimetric curve is asymmetric compared to the theoretical curve. (Panel D) The endotherm of G-actin is fit into the two independent two-state model. Curves 1, 2, 3, and 4 are the experimental endotherm, the least-squares fit of the two-domain model, the melting of the first domain, and the melting of the second domain, respectively. See text for details.

Table I: Deconvolution of Calorimetric Endotherms of G-Actin[a]

	T_m (°C)	ΔH_{cal} (kcal/mol)	ΔH_{vH} (kcal/mol)	ΔG(23 °C) (kcal/mol)	ΔS [cal/(mol·K)]
(1) One-Step Cooperative Transition					
	57.2 ± 0.5	142 ± 5	94 ± 4	10.3	178
(2) Independent Two Two-State Transitions					
transition I	52.3	44 ± 5		3.6	84
transition II	56.7	107 ± 10		8.4	151
(3) Sequential Two Steps (Each Step a Two-State Transition)					
transition I	52.9	54 ± 5		4.1	98
transition II	56.7	96 ± 8		7.2	119

[a] The deconvolution followed the procedure of Freire and Biltonen (1978). Each experimental value is the mean of at least five determinations. The standard deviation is given for each experimental value. The ΔC_p of heat denaturation was 2.3 ± 0.6 kcal/mol. In the calculation of the ΔG(23 °C) of unfolding, a ΔC_p of 2.3 kcal/mol was used. One-third of this value was assigned to transition I and two-thirds to transition II. A heating rate of 0.5 K/min was used in all DSC measurements. Protein concentration ranged between 2.2 and 3.4 mg/mL.

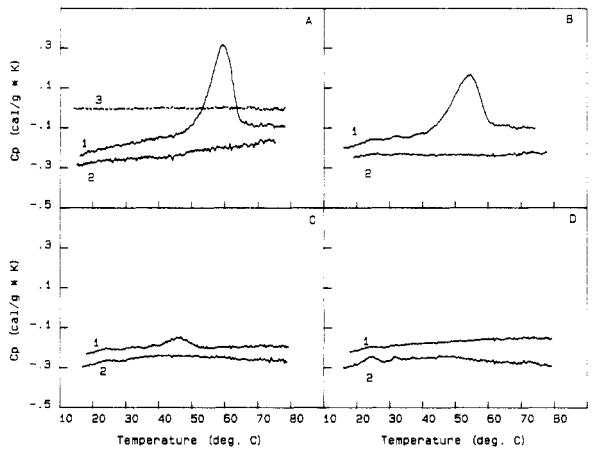

FIGURE 2: Effect of calcium on the thermal stability of G-actin. (Panel A) Curve 1, first-scan endotherm of 3.4 mg/mL G-actin in 2 mM HEPES, 0.2 mM ATP, 0.2 mM $CaCl_2$, and 0.5 mM mercaptoethanol, pH 8.0; curve 2, second-scan of the same sample; curve 3, DSC run of the buffer alone. (Panel B) Curve 1, first scan of 3.52 mg/mL G-actin in the same buffer composition as in panel A, except that the concentration of free calcium was 1.0×10^{-9} M, using the Ca^{2+}/EGTA system; curve 2, second scan of the same sample. (Panel C) Curve 1, DSC run of 3.37 mg/mL G-actin as above except that the free calcium concentration was 2.5×10^{-11} M; curve 2, second scan of the same sample. (Panel D) Curve 1, DSC run of 3.68 mg/mL G-actin in the same buffer as above except that 2 mM EGTA was included so that the free calcium concentration was 1×10^{-11} M; curve 2, second scan of the same sample.

Table II: Calorimetric Enthalpy as a Function of Free Calcium Concentration[a]

free $[Ca^{2+}]$ (M)	ΔH_{cal} (kcal/mol)	T_m (°C)	[EGTA] (mM)	$[CaCl_2]$ (mM)
2×10^{-4}	141 ± 5	59.2 ± 0.1	NB[b]	NB
1×10^{-7}	122 ± 8	53.4 ± 0.6	0.5	0.49
1×10^{-9}	120 ± 6	53.2 ± 0.3	1.0	0.98
1×10^{-10}	119 ± 10	53.2 ± 0.2	1.0	0.83
8×10^{-11}	110 ± 11	53.1 ± 0.8	1.0	0.80
5×10^{-11}	81 ± 10	53.0 ± 0.2	1.0	0.72
2.5×10^{-11}	18 ± 8	47.0 ± 1.0	1.0	0.56
2.3×10^{-11}	15 ± 8	46.0 ± 0.5	1.0	0.21

[a] The free $[Ca^{2+}]$ was determined by using $\log K = 10.7$ for EGTA (Schmidt & Reilly, 1957), where K is the association constant of EGTA and Ca^{2+}. Protein concentration varied from 3.1 to 4.3 mg/mL, using four different protein preparations. The heating rate was 1 K/min. The calorimetric enthalpy is the average of at least three determinations ± the standard deviation. [b] Not buffered.

run. The calorimetric enthalpy is strongly dependent on the free Ca^{2+} concentration. For the free Ca^{2+} concentration between 1×10^{-10} and 1×10^{-7} M, the ΔH_{cal} was rather constant and is approximately 120 ± 5 kcal/mol at a T_m 53 °C (in buffer A with Ca^{2+}/EGTA and at a 1 K/min heating rate). When the free Ca^{2+} concentration was further lowered, a gradual reduction of the calorimetric enthalpy and a complete loss of the transition were observed at a free $[Ca^{2+}]$ of 1×10^{-11} M. There was also a slight shift of the peak temperature from 53 to 47 °C. A plot of calorimetric enthalpy vs free $[Ca^{2+}]$ is shown in Figure 3A. The numerical values are given in Table II. In Figure 3B, a plot based on eq 1 is shown and from the slope of the curve, a Δn of 3.5 was obtained. This result suggests that upon the thermal unfolding there is a release of three to four tightly bound calciums.

Higher free $[Ca^{2+}]$, in 5 mM range, induced a partial polymerization of G-actin as reflected by the increase in viscosity. Formation of oligomers was detected by using nondenaturing polyacrylamide gels. This polymerization seems to be responsible for the gradual shift of the T_m toward the T_m of F-actin and the sharpening of the DSC endotherm, approaching the characteristics of the fully polymerized F-actin.

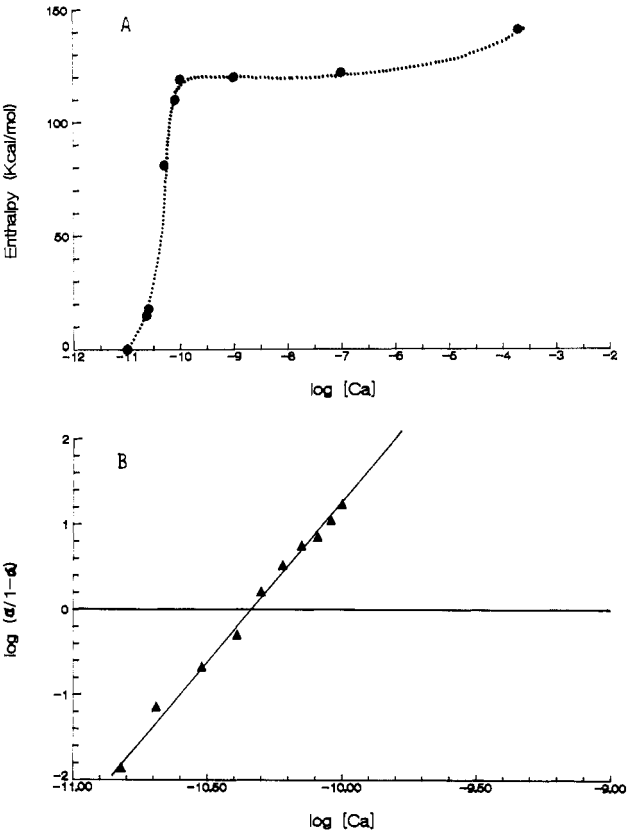

FIGURE 3: Dependence of the calorimetric enthalpy of G-actin on the free calcium concentration. (Panel A) ΔH_{cal} is plotted against the free calcium concentration. (Panel B) The difference in the number of high-affinity calciums bound to the D and N forms of actin was estimated to be 3.5, using eq 1.

EGTA-denatured D-actin did not show a cooperative transition upon thermal denaturation (Figure 2D, curve 1). The CD spectrum (Figure 4A, spectrum 2) and the fluorescence spectrum (Figure 5B, spectrum 3) of EGTA-denatured D-actin resemble those of heat-denatured D-actin (Figure 4A, spectrum 3 for CD, and Figure 5B, spectrum 2 for fluorescence) when the two forms were compared at the same temperature, 25 °C.

Helical Content of the Native and Denatured Structures. Figure 4A reports CD spectra of native actin (curve 1), heat-denatured actin (curve 2), EGTA-denatured actin (curve 3), and fully unfolded U-actin [with 8 M urea or 5 M guanidinium chloride (curve 4)]. A value of $[\theta]_{222}$ obtained for native G-actin was −13 500 ± 500 deg/(cm²·dmol), which corresponds to about 33.6% helix [a complete helix has the value of −38 500 deg/(cm²·dmol) at 222 nm (Nagy & Strzelecka-Golaszewaska, 1972)] or to 29.8% when the whole spectrum was fitted with a least-squares fitting procedure using the spectra reported by Chang et al. (1978) as reference. The value we report is in agreement with that reported by Wu and Yang (1976) and Strzelecka-Golaszewska et al. (1985). The spectrum was characterized by a lower value at 210 nm than at 222 nm. A spectrum of heat-denatured G-actin was characterized by a minimum at 215 nm, and the signal at 222 nm decreased to −8200 deg/(cm²·dmol) which corresponds to about 21% helical structure as compared to the value above, or to 18% residual helix using the least-squares fit. A loss of 37.5% of the native helical structure (or of 39.6% with the computer fitting) was attributed to the irreversible thermal denaturation observed calorimetrically. The EGTA D-actin shows a similar reduction in the ellipticity at 222 nm, and the

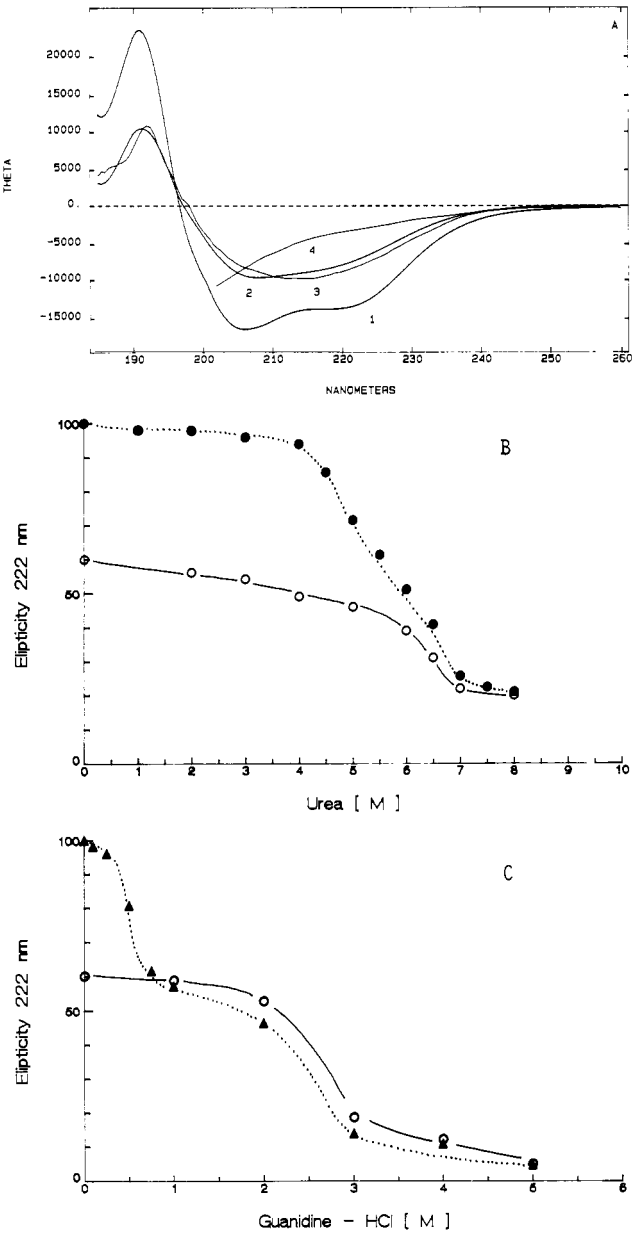

FIGURE 4: Ultraviolet circular dichroism (CD) of actin in different forms. (Panel A) Shown are the CD spectra of native G-actin (1), EGTA-denatured D-actin (2), heat-denatured D-actin (3), and unfolded U-actin, either in 5 M guanidinium chloride or in 8 M urea (4). In all cases, the protein concentration was 1 mg/mL in 2 mM Tris-HCl, 0.2 mM ATP, 0.5 mM Mercaptoethanol, and 0.2 mM Ca^{2+}, pH 8.0 except for curve 2 where 2 mM EGTA was substituted for 0.2 mM Ca^{2+}. All spectra were taken at room temperature (23 °C). See text for details. (Panel B) Urea unfolding of G-actin (●) and EGTA D-actin (○). Both transitions were monophasic, with a midpoint of unfolding (C_m) at 5.52 M for G-actin and of 6.25 M for EGTA D-actin. These measurements were done at 23 °C. (Panel C) Guanidinium chloride unfolding of G-actin (▲) and EGTA D-actin (○). unfolding of G-actin was biphasic. In the first step, 40% of the native helical structure was lost (C_m of 0.44 M). The C_m of the second step occurred at 2.3 M compared to that of EGTA D-actin at 2.4 M. See text for details. Experiments were done at 23 °C.

spectrum appeared nearly identical with that of the heat D-actin.

The remaining 62% of the native helical structure could not be removed by heating to 90 °C, but was fully removed by 5 M guanidinium chloride or 8 M urea (curve 4). Elimination of the guanidinium chloride reversed the CD spectrum to that of the heat-denatured, but not to that of the native structure. In our experiments, this guanidinium chloride exposed protein was unable to polymerize after removal of the denaturant. Unfolding with urea showed a better reversibility to N-actin.

Unfolding of G-actin using urea (Figure 4, panel B) was quite different from the unfolding using guanidinium chloride (curve 1 of Figure 4, panel C). The unfolding by urea appeared broad and monophasic whereas the unfolding by guanidinium chloride clearly was a two-step process. The first transition was completed at 1 M guanidinium chloride, and the second transition had a midpoint at 2.4 M. EGTA D-actin did not show the first transition, and the transition observed (curve 2 of Figure 4, panel C) was superimposable to the second transition of G-actin. The free energies of denaturation presented in Table III are calculated by extrapolating to zero denaturant concentration, $\Delta G°_{app}$ according to Pace (1975). At 23 °C, the apparent change in free energy was 13.0 kcal/mol for the transition from N-actin to U-actin and 9.6 kcal/mol for the transition from D-actin to U-actin when unfolded with urea. When guanidinium chloride was used for unfolding, the apparent free energy was 2.4 kcal/mol for the transition from N-actin to D-actin and 11.3 kcal/mol for the transition from D-actin to U-actin. Since the enthalpy change was not detected for the last transition (D to U) using DSC, the entropy change was calculated to be −31 and −38 cal/(mol·K) at 23 °C, for urea and guanidinium chloride unfolding, respectively.

Tryptophan Fluorescence. The intrinsic fluorescence of G-actin was measured continuously as a function of temperature with an approximate scan rate of 0.7–0.8 K/min. The major contributor to the fluorescence of the protein comes from Trp residues [see also Lehrer and Kerwar (1973)], and the fluorescence intensity was, thus, measured at 335 nm (excited at 290 nm). A cooperative transition was detected which was accompanied by a reduction in the fluorescent intensity, with a T_m of 56.7 °C (Figure 5, panel A). The van't Hoff enthalpy calculated from the fluorescence melting curve was 34 kcal/mol, which is less than one-fourth the ΔH_{cal} and one-third of the ΔH_{vH} calculated from the DSC endotherm. Experiments with heat- and EGTA-treated D-actin did not show sharp transitions in fluorescence over the temperature range from 10 to 85 °C, but rather a continuous reduction in intensity with increasing temperature. The fluorescence intensity of a tryptophan solution was found to have a strong temperature dependence although a spectral shift was not observed [see also Brand et al. (1962)]. Spectral shift is a more sensitive indication of the fluorophore microenvironment. We observed, in agreement with Lehrer and Kerwar (1972), that the Trp emission maximum of N-actin (325 nm) was shifted to 335 nm in heat and EGTA D-actin (Figure 5, panel B). Further shift of the emission maximum to 345 nm was seen for the urea or the guanidinium chloride U-actin (Figure 5, panel B). Heating D-actin up to 80 °C did not cause a red shift of the Trp fluorescence, and the maximum remained at 335 nm (Figure 5, panel C). However, a complete unfolding by guanidinium chloride or urea of D-actin caused the maximum to shift from 335 to 345 nm (Figure 5, panel D).

The fluorescent probe ANS was used to monitor conformational changes. ANS fluorescence increases in intensity when bound to hydrophobic regions of the protein (Stryer 1965). The temperature dependence of the binding is shown in Figure 6. Relatively low ANS accessibility was observed when the protein was in the native state (calculated bound ANS was 9 M/M at 23 °C). Upon heating, the intensity increased, coinciding with the observed thermal transition detected by DSC and Trp fluorescence (Figure 6, panel A). When the solution was cooled, the intensity of ANS fluorescence stayed at a level much higher than the initial value.

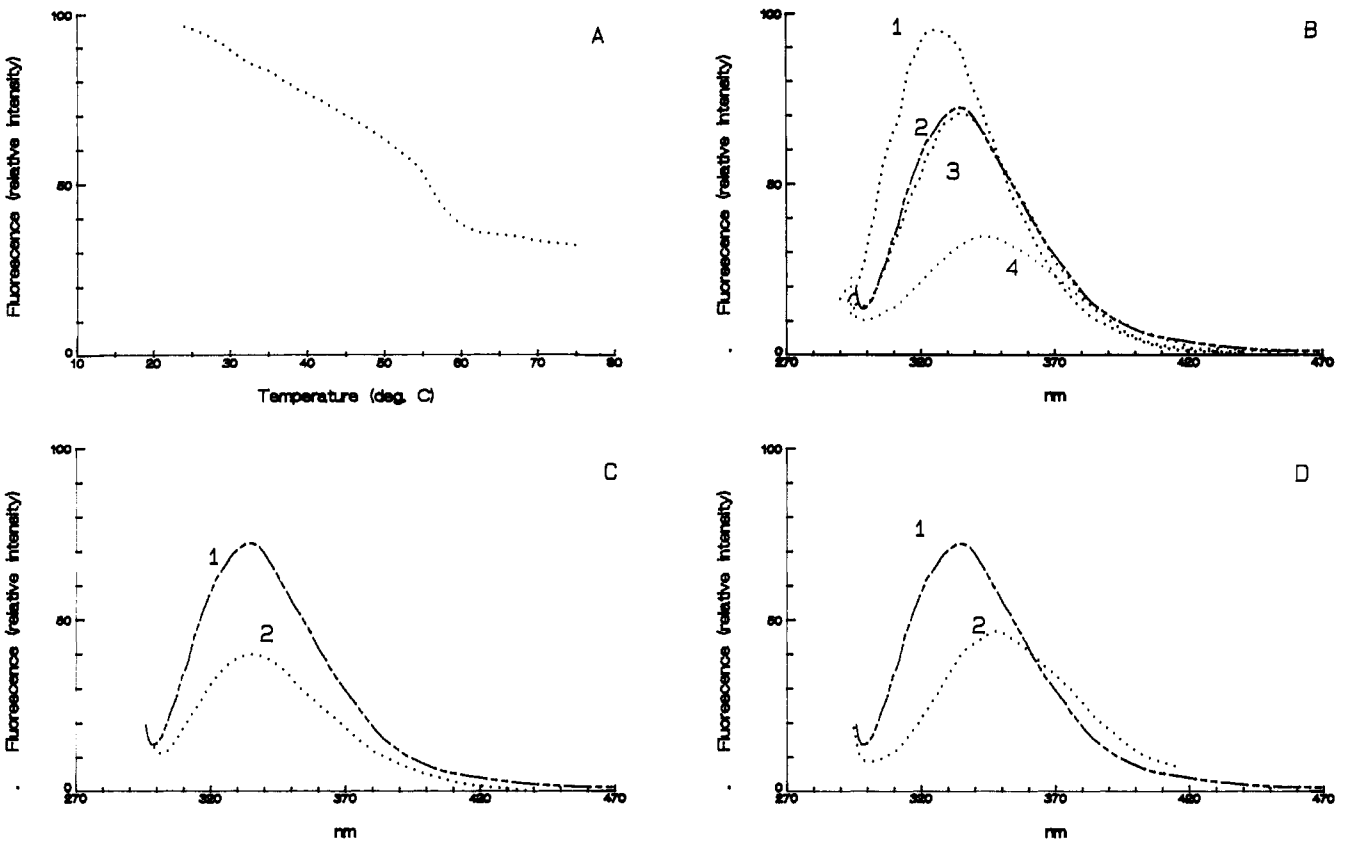

FIGURE 5: Intrinsic tryptophan fluorescence of actin. (Panel A) Thermal denaturation of G-actin as monitored by the intrinsic tryptophan fluorescence. The excitation wavelength was 290 nm, and the fluorescence intensity at 335 nm was followed. The protein concentration was 30 μg/mL, and the heating rate was 0.75 K/min. (Panel B) The emission spectra of native G-actin (1), heat D-actin (2), EGTA D-actin (3), and U-actin in 8 M urea (4). All spectra were taken at 20 °C, with an excitation wavelength of 290 nm. The emission maxima were 325, 335, and 345 nm, respectively, for G-, D-, and U-actin at a protein concentration of 30 μg/mL. (Panel C) Comparison of the emission spectra of heat D-actin at 70 °C (2) and the same sample after cooling to 20 °C (1). The emission maxima for both occurred at 335 nm. The result indicates that although heat denaturation destroyed the hydrophobic core of G-actin, tryptophan residues of the protein are not completely exposed to the solvent. (Panel D) Comparison of the emission spectra of heat D-actin before (1) and after (2) unfolding by 8 M urea (U-actin). A red shift from 335 to 345 nm was obtained at 20 °C.

Table III: Energetics of Actin Unfolding by Urea and Guanidinium Chloride

	urea			guanidinium chloride		
	$\Delta G°_{app}$ (kcal/mol)	C_m (M)	m [kcal/(mol·M)]	$\Delta G°_{app}$ (kcal/mol)	C_m (M)	m [kcal/(mol·M)]
N-actin to U-actin	13.0	5.52	2.35			
N ↔ D transition				2.4	0.44	5.5
D ↔ U transition				10.6	2.30	4.6
D-actin[a] to U-actin	9.6	6.25	1.54	11.3	2.40	4.7

[a] The starting sample is the EGTA- or heat-denatured D-actin at 23 °C. $\Delta G°_{app}$, C_m, and m are the free energy of denaturation extrapolating to zero denaturant concentration, the midpoint of denaturation, and a linear extrapolation constant, respectively. These parameters are obtained by using the model of Pace (1975) and Tanford (1968). The parameter, $m = \Delta G°_{app}/C_m$ has the physical meaning of the difference in the solvent accessibility of the denatured form and the native form (Schellman, 1978). The ΔS of the D-actin to U-actin transition is −31 cal/(mol·K) and −38 kcal/(mol·K) for urea and guanidinium chloride denaturation, respectively.

ANS titrations were performed for the three forms of actin at 23 °C (Panel B). The number of ANS bound for D-actin reached about 50 M/M, at 23 °C, as estimated by Scatchard plot analysis. The binding constant was calculated to be 24 and 30 μM for native actin and heat D-actin, respectively. The emission maximum shifted from 540 nm for free ANS to 470 nm for bound ANS, indicating that the binding sites of ANS were hydrophobic (Turner & Brand, 1968).

Discussion

The thermal denaturation of G-actin is complex. The van't Hoff enthalpy (94 kcal/mol) is much smaller than the calorimetric enthalpy (142 kcal/mol), suggesting that there are at least two structural domains of different thermal stabilities in the molecule. Our data were analyzed by assuming either that the two domains can melt independent of each other or that they melt sequentially one after the other. Distinction between the two models is not feasible based alone on the DSC data. However, we favor the independent melting model because this model produces enthalpy of denaturation for two transitions proportional to the size of the two domains produced when actin is subject to mild proteolytic digestion (Jacobson & Rosenbush, 1976). Polymerization of G-actin to F-actin results in increased thermal stability and a higher degree of cooperativity, with a cooperative ratio changing from 0.70 to 1.4. This implies an interaction among actin monomers in the filament.

Our experiment has established several points. First, the removal of the high-affinity calcium by EGTA completely abolishes the DSC-detectable conformational transition, yet CD analysis suggests that 60% of the native helix content is still preserved. This indicates that the high-affinitive Ca^{2+}

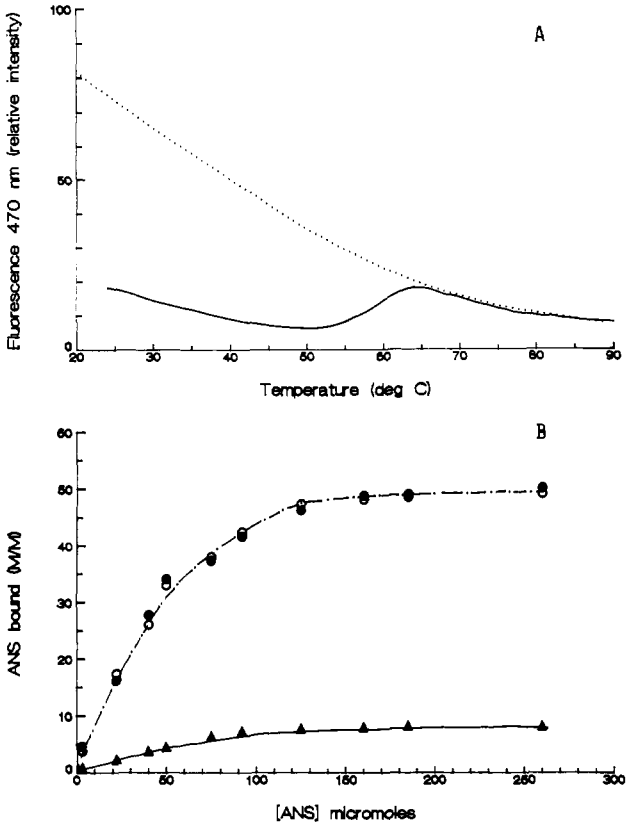

FIGURE 6: Binding of ANS to actin. (Panel A) Heating curve (—) and cooling curve (···) of a solution containing 40 μg/mL G-actin and 30 μg/mL ANS. The excitation wavelength was 400 nm, and the emission was monitored at 470 nm. The heating and cooling rate was approximately 1.25 K/min. (Panel B) ANS binding to native G-actin (▲), heat-denatured D-actin (●) and EGTA D-actin (○). The actin concentration was 30 μg/mL, and the titration was done at 23 °C. Scatchard analysis was used to estimate the binding constant of ANS and the number of binding sites.

stabilizes the enthapy-dependent structure, presumably through van der Waals contacts, of the G-actin. Second, the heat-denatured D-actin resembles the EGTA D-actin, also retaining 60% of the native helix content. This "residual" structure cannot be removed by further heating up to 95 °C. We were unable to make a distinction between the two denaturated forms by CD, fluorescence, or DSC experiments discussed in the paper. Third, the tryptophan fluorescence of both the heat- and the EGTA-denatured D-actin indicates that the hydrophobic core of G-actin is not completely exposed to the solvent upon heat or EGTA denaturation. The emission maximum of tryptophan fluorescence and the ANS binding ability of D-actin suggest preservation of certain hydrophobic environments in the D-actin. Fourth, D-actin can be completely and reversibly unfolded by guanidinium chloride and urea. This unfolding is purely an entropic process. These results can be represented by a simple mechanism for the unfolding of G-actin:

$$\text{N-actin} \rightarrow \text{D-actin} \rightleftharpoons \text{U-actin}$$

The first step is enthalpic and involves the denaturation of two independent domains, of approximately 11 and 31 kDa. The second step completely unfolds the protein and is purely entropic. The possibility that this second step arises from melting of a third stable, independent domain cannot be excluded.

The integrity of N-actin requires high-affinity Ca^{2+}. Loss of these calciums results in the irreversible denaturation to D-actin. We have attempted to quantitate the number of high-affinity Ca^{2+} by using calorimetry (Figure 3) and the Arsenazo III assay. However, the two methods were not consistent; the calorimetric method gave a Δn of 3.5 whereas the Arsenazo III assay gave a Δn of 0.95. It is plausible that the high-affinity Ca^{2+}, when released, could still remain bound to the denatured protein with a relatively high affinity. In this case, the bound Ca^{2+} would be detected by DSC but not by the Arsenazo III assay. Konno and Morales (1985) reported a high-affinity Ca^{2+} with a K_D of 5 nM for actin labeled with *N*-(5-fluoresceinyl)maleimide. Estes et al. (1987) use the calcium-specific chelator Quin2 to study this high-affinity calcium. Carlier et al. (1986) also reported a high-affinity calcium (K_D of 2.6 nM) in G-actin. Our result with Arsenazo III assay agrees with these results.

The D-actin might be considered one of the different types of folding/unfolding intermediates discussed by many authors, e.g., the framework of Kim and Baldwin (1982) or the molten globule of Dolgikh et al. (1981, 1984, 1985). It has a high helix content (19%), and despite the exposure of hydrophobic residues, the protein still maintains a compact structure as evidenced by its ability to bind ANS and the fact that the tryptophan residues are still in a relatively hydrophobic environment. Unfortunately, attempts to recover N-actin from D-actin either by removing guanidinium chloride or by lowering the temperature were not successful. Likewise, the high-affinity Ca^{2+} when released by EGTA could not be restored by the removal of EGTA and the addition of calcium back to the solution. In contrast, the D-actin to U-actin transition is fully reversible.

Analysis of the results of guanidinium chloride is clearly a two-step process. The first transition apparently is related to the N-actin → D-actin denaturation step, and the second is superimposable onto the D-actin → U-actin unfolding step. For the guanidinium chloride unfolding, the free energy of the first denaturation at 23 °C (N-actin → D-actin is 2.4 kcal/mol, and that for the second step (D-actin → U-actin) is 10.6 kcal/mol (Table III). For the urea unfolding from D-actin to U-actin, the free energy change is 13.0 kcal/mol (Table III).

The ΔS of the N-actin to D-actin transition has a positive value of approximately 200 cal/(mol·K) (Table I) whereas that of the D-actin to U-actin transition is negative, −31 cal/(mol·K) by guanidinium chloride unfolding and −38 cal/(mol·K) by urea unfolding (Table III). The ΔS of N-actin to U-actin would be approximately 165 cal/(mol·K). Conversely, folding of U-actin to N-actin would have a negative entropy change of 165 cal/(mol·K). This simple analysis suggests that the stability of N-actin does not depend on the entropy term but rather on the enthalpy term. Our result, however, shows that there is an intermediate state in the folding of U-actin, i.e., D-actin, and that the stability of this intermediate is entropic. No enthalpy contributes to the stability of D-actin.

ACKNOWLEDGMENTS

We thank Drs. D. Shortle and G. L. Nelsestuen for the use of the CD polarimeter and spectrofluorometer, respectively. C. J. Gross kindly helped us in the preparation of the manuscript.

Registry No. Ca, 7440-70-2; urea, 57-13-6; guanidinium chloride, 50-01-1.

REFERENCES

Baldwin, R. L. (1986) *Proc. Natl. Acad. Sci. U.S.A. 83*, 8069–8072.

Brand, L., Everse, J., & Kaplan, N. O. (1962) *Biochemistry 1*, 432–434.

Carlier, M.-F., Pantaloni, D., & Korn, E. D. (1986) *J. Biol. Chem. 261*, 10778–10784.

Chang, C. T., Wu, C.-S. C., & Yang, J. T. (1978) *Anal. Biochem. 91*, 13–31.
Dolgikh, D. A., Gilmanshin, R. I., Brazhnikov, E. V., Bychkova, V. E., Semisotnov, G. V., Venyaminov, S. Y., & Ptitsyn, O. B. (1981) *FEBS Lett. 136*, 311–315.
Dolgikh, D. A., Kolomiets, A. P., Bolotina, I. A., & Ptitsyn, O. B. (1984) *FEBS Lett. 165*, 88–92.
Dolgikh, D. A., Abaturov, L. V., Bolotina, I. A., Brazhnikov, E. V., Bychkova, V. E., Gilmanshin, R. I., Lebedev, O. Y., Semisotnov, G. V., Tiktopulo, E. I., & Ptitsyn, O. B. (1985) *Eur. Biophys. J. 13*, 109–121.
Edge, V., Allewell, N. M., & Sturtevant, J. M. (1985) *Biochemistry 24*, 5899–5906.
Estes, J. E., Selden, L. A., & Gershman, L. C. (1987) *J. Biol. Chem. 262*, 4952–4957.
Freire, E., & Biltonen, R. L. (1978a) *Biopolymers 17*, 463–479.
Freire, E., & Biltonen, R. L. (1978b) *Biopolymers 17*, 481–496.
Freire, E., & Biltonen, R. L. (1978c) *Biopolymers 17*, 497–510.
Jacobson, G. R., & Rosenbush, J. P. (1976) *Proc. Natl. Acad. Sci. U.S.A. 73*, 2742–2746.
Kendrick, N. C., Ratzlaff, R. W., & Blaustein, M. P. (1977) *Anal. Biochem. 83*, 433–450.
Kim, P. S., & Baldwin, R. L. (1982) *Annu. Rev. Biochem. 51*, 459–489.
Konno, K., & Morales, M. F. (1985) *Proc. Natl. Acad. Sci. U.S.A. 82*, 7904–7908.
Laemmli, U. K. (1970) *Nature (London) 277*, 680–685.
Lehrer, S. S., & Kerwar, G. (1972) *Biochemistry 11*, 1211–1217.
Lippert, E. (1957) *J. Electrochem. Soc. 61*, 962.
Lowry, D. H., Rosebrough, N. J., Farr, A. R., & Randell, R. J. (1951) *J. Biol. Chem. 193*, 265–275.
Nagy, B., & Jencks, P. W. (1962) *Biochemistry 1*, 987–996.
Nagy, B., & Strzelecka-Golaszewska, H. (1972) *Arch. Biochem. Biophys. 150*, 428–435.
Pace, C. N. (1975) *CRC Crit. Rev. Biochem. 3*, 1–43.
Pardee, J. D., & Spudich, J. A. (1982) *Methods Enzymol. 85*, 164–181.
Privalov, P. L. (1982) *Adv. Protein Chem. 35*, 1–104.
Privalov, P. L., & Potekhin, S. A. (1986) *Methods Enzymol. 131*, 4–51.
Privalov, P. L., & Gill, S. J. (1988) *Adv. Protein Chem. 39*, 191–234.
Privalov, P. L., Griko, Y. V., & Venyaminov, S. Y. (1986) *J. Mol. Biol. 190*, 487–498.
Schellman, J. (1978) *Biopolymers 17*, 1305–1322.
Schmidt, R. W., & Reilley, C. N. (1957) *Anal. Chem. 29*, 264–268.
Strezelecka-Golaszewska, H., Veniaminov, S. Y., Zmorzynsky, S., & Mossakowska, M. (1985) *Eur. J. Biochem. 147*, 331–342.
Stryer, L. (1965) *J. Mol. Biol. 13*, 482–495.
Sturtevant, J. M. (1987) *Annu. Rev. Phys. Chem. 38*, 463–488.
Tanford, C. (1968) *Adv. Protein Chem. 23*, 121–275.
Takahashi, K., Casey, J. L., & Sturtevant, J. M. (1981) *Biochemistry 20*, 4693–4697.
Tatunashvili, L. V., & Privalov, P. L. (1984) *Biofizika 29*, 583–585.
Tsalkova, T. N., & Privalov, P. L. (1985) *J. Mol. Biol. 181*, 533–544.
Tsong, T. Y., Hearn, R. P., Wrathall, D. P., & Sturtevant, J. M. (1970) *Biochemistry 9*, 2666–2677.
Turner, D. C., & Brand, L. (1968) *Biochemistry 7*, 3381–3390.
West, J. J., Nagy, B., & Gergely, J. (1967) *Biochem. Biophys. Res. Commun. 29*, 611–616.
Wu, C.-S. C., & Yang, J. T. (1976) *Biochemistry 15*, 3007–3014.